Catalytic, Enantioselective Aldol Reaction with an Artificial Aldolase Assembled from a Primary Amine and an Antibody

Jean-Louis Reymond*,† and Yuanwei Chen

Department of Molecular Biology, MB-11, The Scripps Research Institute, 10666 North Torrey Pines Road, La Jolla, California 92037

Received May 3, 1995®

The aldol addition of acetone to aldehydes **1**–**5** is catalyzed by primary amine **14**. The pH profile is consistent with catalysis by the free amine, with $pK_a = 8.55$ for its conjugate acid. The catalytic cycle involves rate-determining coupling of the aldehyde with enamine **III** formed by condensation of the amine and acetone. Condensation with the aldehyde to form imine **16** inhibits catalysis ($K_{16} = 7.8$ mM). Assembly of amine **14** with an antibody against quaternary ammonium hapten **19** yields an artificial aldolase which catalyzes the reaction. The catalyst is approximately 600 times more reactive than amine **14** alone. The pK_a of the amino group is unchanged within the complex. The antibody catalyzes the formation of amino nitrile **17** in the presence of cyanide, suggesting that condensation of acetone with amine **14** is favored by complexation with the antibody, an effect which might account for catalysis. The reaction with aldehyde **1** is *si* enantioface selective and gives aldol (*SS*)-**6** (>95% de) from (*S*)-**1** and aldol (*RS*)-**6** from (*R*)-**1** (65% de) in a 1:2.8 ratio. These experiments show the principles of a novel approach for the design of an artificial aldolase.

Introduction

The aldol condensation is one of the most important bond-constructing processes in synthetic chemistry. Although very efficient methods have been developed for aldol condensations using stoichiometric amounts of enol or enolate species,[1] one of the most impressive techniques involves direct coupling of ketones with aldehydes in aqueous medium using aldolase enzymes.[2] In this case the nucleophilic enol species is generated in catalytic amounts, so that the method is extremely economical in energetic terms, as no chemical energy is spent for coupling other than mixing both components together. Excellent stereochemical control is achieved by these enzymes, which give access to optically pure aldol products in preparative scale.

The example of type I aldolase enzymes,[3] which use the ϵ-amino group of a lysine residue as a key catalytic group to effect enamine-mediated aldol chemistry, suggests that an artificial aldolase should possess a primary amine function of suitable reactivity within its active site. Herein we report upon the assembly of an artificial aldolase from a simple primary amine and a monoclonal antibody. First, catalysis of a model cross-aldolization reaction between acetone and aldehydes **1** to **5** by the simple primary amine **14** via an enzyme-like enamine mechanism is exposed. We then demonstrate the assembly of this amine with an antibody raised against the piperidinium hapten **19** to form an enantioselective artificial aldolase.[4]

Results and Discussion

Synthesis. Aldehydes **1**–**4** were prepared in one step by palladium-catalyzed coupling of 4- and 3-iodoacetanilide with methallyl alcohol or allyl alcohol.[5] Aldehyde **5** was prepared from aldehyde **4** by aldol condensation with excess propanal in aqueous NaOH followed by reduction of the resulting unsaturated aldehyde with H_2/Pd/C. All aldehydes were purified by RP-HPLC for kinetic studies. Authentical samples of the aldol products **6**–**10** were obtained from the reaction of the corresponding aldehydes in 10% acetone in water with NaOH as catalyst and purified by RP-HPLC (Scheme 1).

Products and Kinetics of the Aldol Reaction. Kinetic studies of the reaction were conducted in aqueous buffer (50 mM bicine adjusted with NaOH, 100 mM NaCl) with 1–10% v/v acetone and 0.1–2 mM aldehyde. Under these conditions, a large excess of acetone ensures that the thermodynamic balance of the aldolization lies to the condensation side and allows the reaction to take place at practical rates even at relatively low pH. Aldehydes **1**–**5** were water soluble within the concentration range used, which allowed us to work without cosolvent other than the added acetone. The reaction was conveniently followed by analytical RP-HPLC using detection of the acetanilide chromophore by UV at 250 nm (Table 1).

In diluted NaOH with 5% v/v acetone and 0.25 mM aldehyde at 20 °C, aldehyde **1** gave aldol addition product **6**, together with a small amount (<5%) of α,β-unsaturated ketone **11**. The reaction of unbranched aldehyde **2** was more complicated and gave aldol **7**, enone **12**, and unsaturated aldehyde **13** in a 4:1:1 ratio. Due to the much cleaner reaction of aldehyde **1**, kinetic studies were carried out with this substrate.

† Phone: (619) 554-4384. FAX: (619) 554-6778. e-mail: jlouis@scripps.edu.

® Abstract published in *Advance ACS Abstracts*, September 15, 1995.

(1) For recent examples, see: (a) Carreira, E. M.; Lee, W.; Singer, R. A. *J. Am. Chem. Soc.* **1995**, *117*, 3649. (b) Denmark, S. E.; Griedel, B. D.; Coe, D. M.; Schnute, M. E. *J. Am. Chem. Soc.* **1994**, *116*, 7026 and references cited therein.

(2) (a) Gijsen, H. J. M.; Wong, C.-H. *J. Am. Chem. Soc.* **1994**, *116*, 8422. (b) Hupe, D. J. In *Enzyme Mechanisms*; Page, M. I., Williams, A., Eds.; Royal Society of Chemistry, Burlington House: London 1987; p 317–344. (c) Fessner, W.-D. *Kontakte* **1992**, *3*, 3–9.

(3) Hupe, D. J. In *New Comprehensive Biochemistry*, Vol. 6, The Chemistry of Enzyme Action; Page, M. I., Ed.; Elsevier: Amsterdam, 1984; Chapter 8.

(4) A preliminary account of this work has been published in communication format: Reymond, J.-L.; Chen, Y. *Tetrahedron Lett.* **1995**, *36*, 2575.

(5) (a) Chalk, A. J.; Magennis, S. A. *J. Org. Chem.* **1976**, *41*, 273. (b) Review: de Meijere, A.; Meyer, F. A. *Angew. Chem., Int. Ed. Engl.* **1994**, *33*, 2379.

0022-3263/95/1960-6970$09.00/0

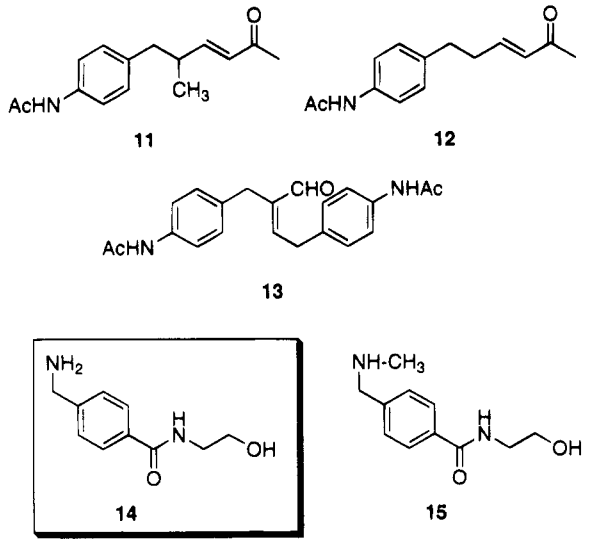

The ^{1}H-NMR spectrum of aldehyde **1** in D_2O shows that 50% of the carbonyl group is present as the *gem*-diol form in water. This equilibrium appears unaffected by the pH (added acid (trifluoroacetic acid) or base (NaOD)). Thus only half of the aldehyde is present as the reactive carbonyl form in water.

In buffered media 7 < pH < 10, the aldol addition of aldehyde **1** to form aldol **6** is first order in acetone up to 8% v/v. It is also first order in aldehyde **1** up to 2 mM. No measurable buffer catalysis is observed (phosphate, bicine, or triethanolamine). The pH profile shows that the reaction is also first order in hydroxide (Figure 1). General bases which accelerate proton exchange of acetone (see below) do not accelerate the reaction, implying that enolization of acetone is a fast preequilibrium established before the rate-limiting step. Since the concentration of enolate is proportional to [OH^-] below the pK_a of the acetone enol (pK_a = 10.83),[6,7] the pH profile is consistent with the rate limiting step being a simple bimolecular coupling between the enolate of acetone and the aldehyde.

Catalysis by Primary and Secondary Amines. Catalysis of the aldol condensation of aldehydes by primary and secondary amines, in particular amino acids, in buffered aqueous medium, was first reported by Fischer and Marschall in 1931.[8] One of the fundamental aspects of this catalysis is the fact that it is only detectable at relatively low pH, where the specific base catalyzed reaction via the enolate is sufficiently slow. However, catalysis of cross-aldolizations between ketones and aldehydes by primary or secondary amines have not been reported, probably because Mannich-type condensation between the aldehyde imine and the ketone was expected to occur preferentially.

Scheme 1. Synthesis of Aldehydes 1 to 5 and Aldol Products 6 to 10

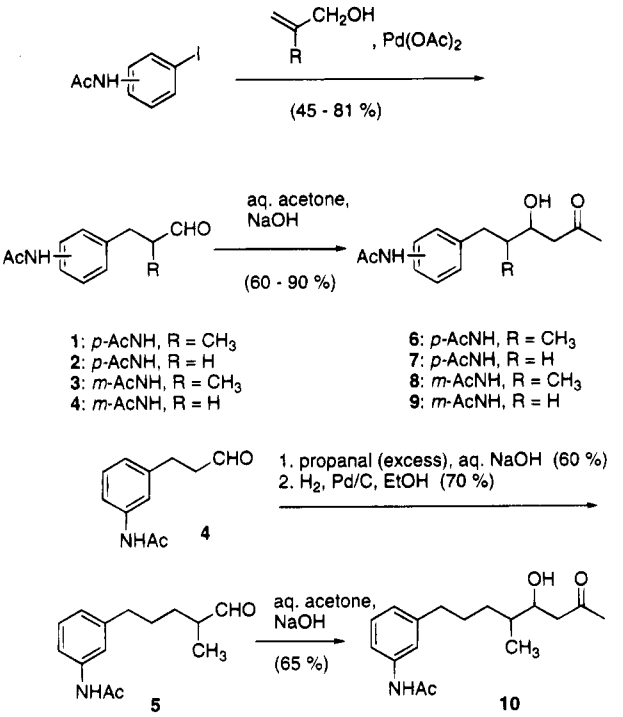

Table 1. HPLC Conditions for Aldol Reactions of Aldehydes 1–5[a]

	% A	% B	t_R(aldehyde), min	t_R(aldol), min
1[b]	75	25	20.5	24.4
2[c]	75	25	5.8	8.2
3[b]	70	30	16.4	26.5
4[c]	75	25	6.9	10.8
5[b]	50	50	13.4	8.8

[a] Isocratic elution at 1.5 mL/min, detection by UV 250 nm, A = 0.1% TFA in H_2O, B = 50/50 CH_3CN/H_2O. [b] Column: Microsorb-MV 86-203-C5, 0.45 × 22 cm. [c] Column: Vydac 218TP54, 0.45 × 22 cm.

We found that cross-aldolization between acetone and aldehydes **1** and **2** was catalyzed by a number of simple primary and secondary amines at pH 8.0, including the amino acids proline and valine, (*S*)-α-methylbenzylamine, ethanolamine, morpholine, methylamine, and dimethylamine. Except for the case of the amino acid proline, which was more efficient than the other amino acids, catalysis was generally more efficient with primary than with secondary amines. Benzylic amine **14** was particularly efficient for this catalysis. The corresponding secondary amine **15**[9] was ten times less efficient.

The pH profile for aldolization catalysis by the primary amine **14** shows a saturation effect (Figure 1). The double reciprocal plot of this data is linear, consistent with catalysis by an ionizable group as free base with $k_{\text{free base}} = 2.0 \times 10^{-4}$ M^{-2} s^{-1} and an apparent pK_a = 8.55 for the dissociation constant for its conjugate acid.[10]

An interesting aspect of this catalysis is shown by the amine concentration profile (Figure 2). Saturation kinetics are observed at high amine concentration. When mixtures of aldehyde **1** and amine **14**, with or without acetone, are examined in buffered D_2O, imine **16** is

(6) (a) Tapuhi, E.; Jencks, W. P. *J. Am. Chem. Soc.* **1982**, *104*, 5758. (b) Chiang, Y.; Kresge, A. J.; Schepp, N. P. *J. Am. Chem. Soc.* **1989**, *111*, 3977.

(7) Chiang, Y.; Kresge, A. J.; Tang, Y. S.; Wirz, J. *J. Am. Chem. Soc.* **1984**, *106*, 460.

(8) For aldol condensations catalyzed by primary and secondary amines in water, see: (a) Fischer, F. G.; Marschall, A. *Ber.* **1931**, *64*, 2825. (b) Langenbeck, W.; Borth, G. *Ber.* **1942**, *75*, 951. (c) Spencer, T. A.; Neel, H. S.; Flechtner, T. W.; Zayle, R. A. *Tetrahedron Lett.* **1965**, 3889. (d) Gutsche, C. D.; Redmore, D.; Buriks, R. S.; Nowotny, K.; Grassner, H.; Armbruster, C. W. *J. Am. Chem. Soc.* **1967**, *89*, 1235. Retroaldol reactions: (e) Westheimer, F. H.; Cohen, H. *J. Am. Chem. Soc.* **1938**, *60*, 90. (f) Westheimer, F. H.; Jones, W. A. *J. Am. Chem. Soc.* **1941**, *63*, 3283. Decarboxylations: (g) Pedersen, K. J. *J. Am. Chem. Soc.* **1938**, *60*, 595. (h) Johnsson, K.; Allemann, R. K.; Widmer, H.; Benner, S. A. *Nature* **1993**, *365*, 530. For amino acid catalysis of an aldol process in nonaqueous medium: (i) Agami, C.; *Bull. Soc. Chim. Fr.* **1988**, *3*, 499 and references cited therein.

(9) Jahangiri, G. K.; Reymond, J.-L. *J. Am. Chem. Soc.* **1994**, *116*, 11264.

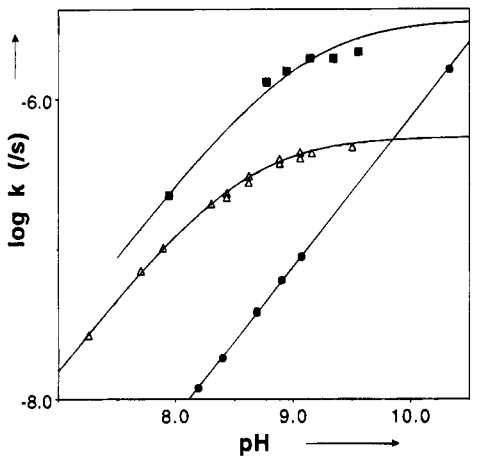

Figure 1. pH profile for the aldol reaction of acetone with aldehyde **1**. Observed first-order rate constant log k (s^{-1}): (●) catalysis by hydroxide with [acetone] = 0.68 M, [**1**] = 400 μM; (△) catalysis by 4 mM amine **14** with [acetone] = 0.68 M, [**1**] = 400 μM; (■) k_{cat} for Ab 72D4 + amine **14**, with [acetone] = 0.136 M, [**1**] = 200 μM, [Ab] = 10 μM. Measured in 50 mM bicine buffer, 100 mM NaCl, 20 °C. The line for hydroxide catalysis is the best linear, fit k_{OH^-} = 0.012 M^{-2} s^{-1}. The saturation lines were calculated from the linear double reciprocal plot of the experimental points (14 points, r^2 = 0.999 for **14**, six points, r^2 = 0.997 for Ab 72D4 + **14**) as $1/k_{app} = 1/k_{max} + (1/[OH^-])(K_b/k_{max})$, which gives k_{max}(**14**) = 2.0 × 10^{-4} M^{-2} s^{-1}, K_b(**14**) = 3.6 × 10^{-6} M. k_{max}(Ab 72D4 + **14**) = 0.123 M^{-2} s^{-1}, K_b(Ab72D4 + **14**) = 1.2 × 10^{-5} M.

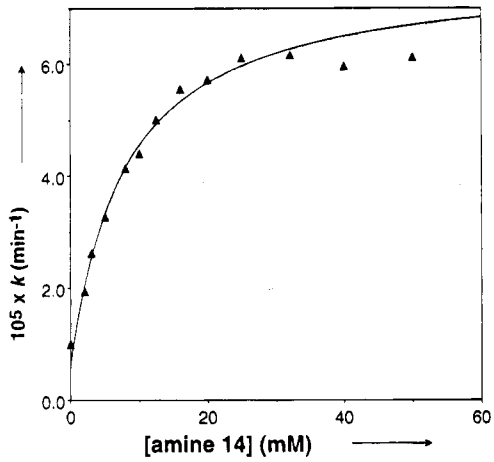

Figure 2. Aldolization rate of aldehyde **1** as a function of amine **14** concentration. Measured at 20 °C in 50 mM bicine, 100 mM NaCl, pH 9.0, 5% v/v acetone, 250 μM **1**. $k_{obs} = k_{net}$(**14**) + $k_{app}(OH^-)$. The line was calculated from the linear double reciprocal plot of the net rate for catalysis by **14** (12 points, r^2 = 0.993) as $1/k_{net}(\mathbf{14}) = 1/(k_{app}(\mathbf{14})K_{16}[\mathbf{1}]_T) + (1/[\mathbf{14}](1/k_{app}(\mathbf{14}))$, giving K_{16} = 7.8 mM and k_{app}(**14**) = 2.2 × 10^{-4} M^{-2} s^{-1}.

detected in addition to free aldehyde **1** and its *gem*-diol. By contrast, the ^{1}H-NMR spectrum of amine **14** in buffered D_2O is unaffected up to 20% v/v acetone, ruling out that saturation could occur by preequilibrium formation of a condensation product with acetone. One can interpret the saturation data as a competitive inhibition effect via formation of imine **16**.[11] A double reciprocal plot of the data gives K_{16} = 7.8 mM for the dissociation constant of the imine, in good agreement with the published value of 11 mM for the condensation equilibrium of isobutyraldehyde with methylamine.[12] Inhibition via imine formation is negligible under our experimental conditions (200 μM aldehyde and 0–2 mM amine).

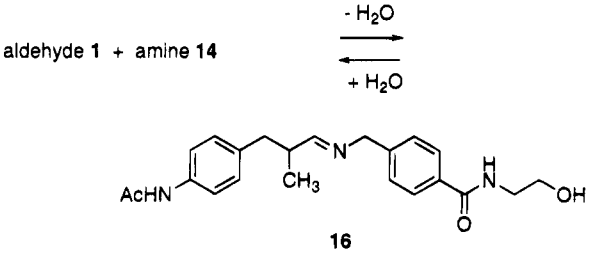

Despite this unfavorable inhibition, the reaction could be carried out in preparative, relatively concentrated solutions by working at higher temperatures. Thus, a solution of 0.1 M aldehyde **1** and 0.1 M amine **14** in buffer at pH 8.0 (50 mM bicine) containing 10% acetone was heated at 80 °C for 5 h, after which approximately 75% of the aldehyde was consumed. Under the same conditions, a control experiment without amine **14** gave less than 2% conversion. The product isolated from the amine-catalyzed reaction (69% yield) consisted of a 1:2 mixture of aldol **6** and its dehydration product enone, **11**. Unreacted aldehyde **1** was also recovered (15% yield). Most significantly, amine **14** was recovered unchanged (90% isolated). The reaction of linear aldehyde **2** was not successful under these conditions. An alternative procedure using higher dilutions and a large excess of methylamine as catalyst at 20 °C for 5 days afforded only partial conversion (50%) of aldehyde **2** to aldol **7** (20% isolated), together with enone **12** (4% isolated) and unsaturated aldehyde **13** (5.5% isolated).

Mechanism of the Amine Catalysis. At this point, two observations suggest an enamine mechanism for aldolization catalysis by primary amine **14**: (1) failure to catalyze the reaction with tertiary amines and buffers, indicating that simple deprotonation catalysis is not involved; (2) the inhibitory effect of the formation of imine **16**, which rules out a Mannich-type condensation mechanism. The enamine mechanism would take place according to the cycle outlined in Scheme 2.[2b]

In enzymatic systems, the presence of an iminium intermediate, which is the direct precursor of the enamine, has been established by trapping either with borohydride to produce a secondary amine or with cyanide to generate, reversibly, a cyanohydrin.[13] When amine **14** was added to a 0.2 M cyanide solution buffered at pH 9 and containing 1–3% v/v acetone, rapid formation of the unstable Strecker product **17** was observed,

(10) There is an apparent lowering of the pK_a compared to the protonated amine **14** (pK_a = 9.15 by titration). This is usually not the case for catalysis involving imine or enamine intermediates because the equilibrium between free amine and imine or enamine, which involves simple elimination of H_2O, is pH independent (see ref 2b). This apparent lowering might be caused by an interference by formation of imine **16** since the measurment was done at [**14**] = 5 mM. The pH profile for aldolization of **2** under catalysis by 1 mM **14** with 5% v/v acetone (pH 7–9.5, eight points, r^2 = 0.999 for double reciprocal plot, data not shown) gives an apparent pK_a = 8.8.

(11) Equation 1: $[\mathbf{1}]_T \times k_{net}(\mathbf{14}) = k_{app}(\mathbf{14}) \times [\mathbf{14}] \times [\mathbf{1}]$, with $[\mathbf{14}]_T = [\mathbf{14}] + [\mathbf{16}]$ and $[\mathbf{1}]_T = [\mathbf{1}] + [\mathbf{16}]$. Under the conditions of the experiment (250 μM **1**), $[\mathbf{1}]_T \ll [\mathbf{14}]_T$, one has $[\mathbf{14}] = [\mathbf{14}]_T$ and $[\mathbf{1}] = [\mathbf{1}]_T - [\mathbf{16}]$. The dissociation constant of imine **16** is $K_{16} = [\mathbf{14}] \times [\mathbf{1}]/([\mathbf{1}]_T - [\mathbf{1}])$, from which $[\mathbf{1}] = K_{16} \times [\mathbf{1}]_T/([\mathbf{14}] + K_{16})$. Replacement of [**1**] with this expression in eq 1 above gives the expression in the legend of Figure 2.

(12) Hine, J.; Menon, B. C.; Jensen, J. H.; Mulders, J. *J. Am. Chem. Soc.* **1966**, *88*, 3367.

(13) (a) Cash, D. J.; Wilson, I. B. *J. Biol. Chem.* **1966**, *241*, 4290. (b) Brand, K.; Horecker, B. L. *Arch. Biochem. Biophys.* **1968**, *123*, 312.

Scheme 2. Enamine Mechanism for Catalysis by Amine 14

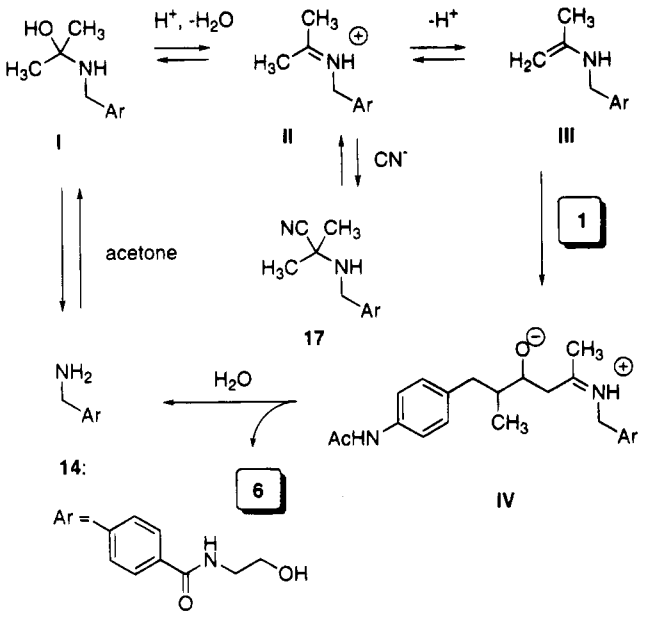

which implied that imminium ion **II** was formed rapidly under the conditions of the aldol reaction.

The role of iminium **II** as a direct precursor for enamine **III** was confirmed by examining the catalysis of acetone enolization by amine **14**. The rate of acetone enolization under catalysis by either a tertiary amine (*N*-methyldiethanolamine) or our primary amine **14** was measured in buffered D_2O (pD = 9.0) by following the decrease of the acetone CH_3 signal by ^1H NMR. Enolization was first order in the tertiary amine under these conditions, reflecting direct deprotonation of acetone by the amine (k_{exch} = 1.7 × 10^{-4} mM^{-1} h^{-1}, Figure 3). In addition to a similar first order term (k_{exch} = 1.8 × 10^{-4} mM^{-1} h^{-1}), primary amine catalysis also showed a second-order term (k^2_{exch} = 8.0 × 10^{-6} mM^{-2} h^{-1}). This term should correspond to deprotonation of imminium **II** by the primary amine and has been studied in detail for the case of primary amine catalysis of β-elimination reactions.[14] Here it provides direct kinetic evidence that iminium **II** enolizes to key enamine **III** under the reaction conditions.

Aldolization of aldehyde **1** to aldol **6** was then followed under the conditions of the enolization experiment above. The tertiary amine had no measurable effect on the reaction rate up to 75 mM. Catalysis by amine **14** was now first order in amine (0.2–2 mM) and was not affected by the concentration of triethanolamine (10–75 mM). This behavior indicates that enolization, or formation of enamine **III** for the enamine mechanism, is not rate limiting for aldolization. Its thus seems reasonable that the rate-limiting step in the amine **14** catalyzed reaction is the addition of enamine **III** to the aldehyde to form adduct **IV**. This mechanism is fully consistent with the kinetic parameters of the amine-catalyzed reaction, which show apparent first order in amine, acetone, and aldehyde.

Assembly of the Artificial Aldolase. Aldolase enzymes function by virtue of an active site lysine residue engaging in enamine formation. The experiments above show that amine **14** possesses in itself all the catalytic features of a primitive aldolase, including a relatively low p*K* which is favorable for such chemistry. What is missing is a better efficiency and the ability to achieve stereoselectivity and chemoselectivity. We reasoned that this might be feasible by noncovalent assembly of this amine with a properly designed antibody pocket, provided that this assembly would simultaneously result in a significant increase in the reactivity of the amine to be observable.

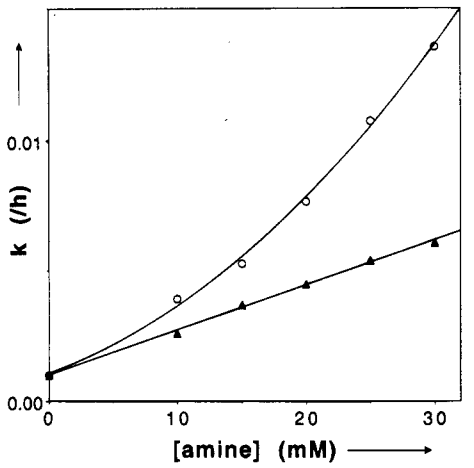

Figure 3. Observed first-order rate constants for proton exchange of acetone-d_0 to acetone-d_6 in D_2O as a function of amine concentration: (○) amine **14**; (▲) *N*-methyldiethanolamine. Measured at 20 °C at pD 9.0 with 100 mM NaCl, 1% v/v acetone. The best linear fit of the experimental points for *N*-methyldiethanolamine gives k_{exch} = 1.7 × 10^{-4} mM^{-1} h^{-1}. The second-order polynomial fit for **14** gives k_{exch}(**14**) = 1.8 × 10^{-4} mM^{-1} h^{-1} and k^2_{exch}(**14**) = 8.0 × 10^{-6} mM^{-2} h^{-1}.

In principle the rate of aldolization depends on the concentration of enamine **III**, which is formed in a rapid preequilibrium. Aldolization catalysis might therefore be improved by placing amine **14** within a hydrophobic environment, which would favor its condensation with acetone by exclusion of water. We investigated possible catalysis by a combination of amine **14** with monoclonal antibodies against four distinct *N*-benzylpiperidine and -pyridine derivatives, **18**–**21** (Scheme 3).[15] These antibodies were expected to assemble with amine **14** by a strong binding interaction at the aromatic group (Ar), which would place the reactive amino group within a hydrophobic environment induced by the hydrophobic envelope of the piperidine or pyridine nitrogen in these haptens.[16] The rate-limiting coupling of enamine **III** to form **IV** is also accompanied by the emergence of a positive charge on the nitrogen center. In that respect, these haptens provided an electrostatically correct model for the transition state of the reaction, following the general principle of transition state analogy employed in the design of catalytic antibodies.[17]

(14) Hupe, D. J.; Kendall, M. C. R.; Spencer, T. A. *J. Am. Chem. Soc.* **1973**, *95*, 2271.

(15) (a) Reymond, J.-L.; Janda, K. D.; Lerner, R. A. *Angew. Chem., Int. Ed. Engl.* **1991**, *30*, 1711. (b) Reymond, J.-L.; Janda, K. D.; Lerner, R. A. *J. Am. Chem. Soc.* **1992**, *114*, 2257. (c) Reymond, J.-L.; Jahangiri, G. K.; Stoudt, C.; Lerner, R. A. *J. Am. Chem. Soc.* **1993**, *115*, 3909. (d) Sinha, S. C.; Keinan, E.; Reymond, J.-L. *J. Am. Chem. Soc.* **1993**, *115*, 4893. (e) Sinha, S. C.; Keinan, E.; Reymond, J.-L. *Proc. Natl. Acac. Sci. U.S.A.* **1993**, *90*, 11910. (f) Koch, A.; Reymond, J.-L.; Lerner, R. A. *J. Am. Chem. Soc.* **1994**, *116*, 803. (g) Reymond, J.-L.; Reber, J.-L.; Lerner, R. A. *Angew. Chem., Int. Ed. Engl.* **1994**, *33*, 475. (h) Chen, Y.; Reymond, J.-L.; Lerner, R. A.; *Angew. Chem. Int. Ed. Engl.* **1994**, *33*, 1607.

(16) Shabat, D.; Itzaky, H.; Reymond, J.-L.; Keinan, E. *Nature* **1995**, *374*, 143.

Scheme 3. Transition State of Amine 14 Catalyzed Aldolization and Related Analogs 18–22 Used for Antibody Production

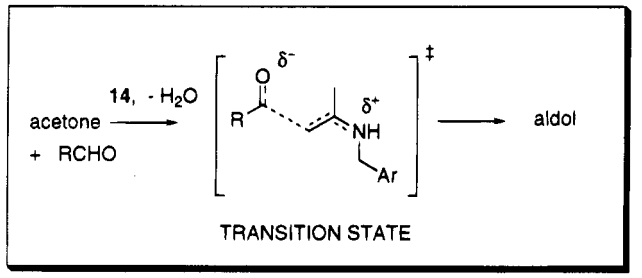

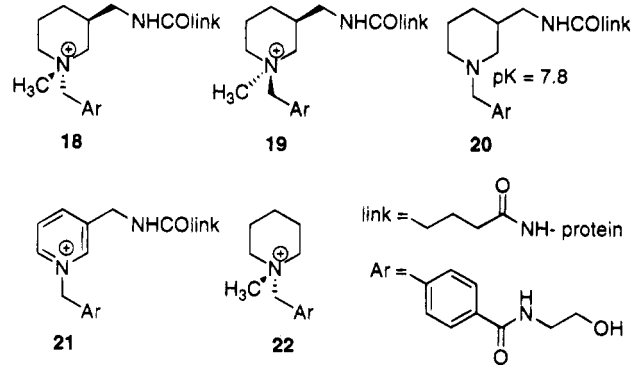

Amine **14** was assayed for catalysis of the formation of aldol **6** from aldehyde **1** and acetone at pH 8.0 in the presence of 86 different monoclonal antibodies obtained from these haptens (22 anti-**18**, 24 anti-**19**, 14 anti-**20**, 26 anti-**21**). Catalysis was observed with three anti-**18** and three anti-**19** antibodies. The catalytic activities were quantitatively inhibited by addition of hapten **22**, demonstrating that amine **14** associated specifically to the antibody combining site. The catalyst assembled from amine **14** and antibody 72D4 (anti-**19**) was characterized in detail.

It was immediately apparent that only the assembled catalyst was active for aldolization. No catalysis was observed using antibody 72D4 without amine **14**. Conversely, catalysis by amine **14** alone was very inefficient at the concentrations sufficient to trigger catalysis of the antibody–amine complex. As was the case for anti-**20** and anti-**21** antibodies, BSA (bovine serum albumin) and three monoclonal antibodies raised against unrelated haptens did not combine with amine **14** to form an active catalyst, clearly excluding that catalysis might arise from a nonspecific adsorption on the protein surface. Indeed the inhibition observed with hapten **22** implied that the interaction with the amine was taking place in the antigen binding site of the antibody.

Characterization of the Antibody–Amine Catalytic Complex. Michaelis–Menten kinetics were observed with respect to amine **14** at fixed concentrations of both acetone and aldehyde **1**, giving K_D = 340 μM for the apparent dissociation constant of the active catalyst (Ab 72D4 + amine **14**). Aldehydes **2**–**5** were also accepted as substrates. Kinetic analysis gave similar dissociation constants K_D for the antibody–amine complex using these aldehydes (Figure 4). It also showed

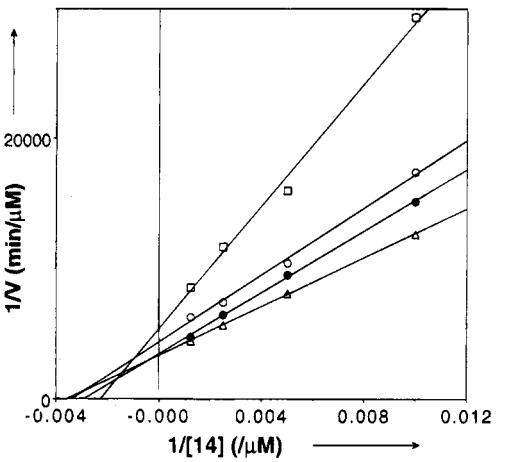

Figure 4. Double reciprocal plot of the rate of aldolization under catalysis by antibody 72D4 + amine **14** as a function of amine **14** concentration. The apparent dissociation constant K_D for the complex is given by the x-intercept as $(-1/K_D)$. Measured at 20 °C in 50 mM bicine, pH 8.0, 100 mM NaCl, with 1% v/v acetone, 10 μM antibody, 200 μM aldehyde (●) **1**, (△) **2**, (□) **3**, (○) **4**.

Table 2. Kinetic Parameters for Antibody 72D4 + Amine 14[a]

substrate, pH	K_M, mM	k_{cat}, s^{-1}	k_{cat}/K_M,[b] $M^{-1}\,s^{-1}$	k_{uncat},[c] $M^{-1}\,s^{-1}$	k_{cat}/k_{uncat}, M
1, 8.0	1.8	3.0×10^{-6}	1.7×10^{-3}	2.9×10^{-8}	100
1, 9.3	1.4	1.2×10^{-5}	1.1×10^{-2}	2.0×10^{-7}	60
2, 8.0	4.9	8.3×10^{-6}	1.6×10^{-3}	4.9×10^{-8}	170
3, 8.0	1.9	1.6×10^{-6}	8.4×10^{-4}	2.4×10^{-8}	67
4, 8.0	3.3	3.9×10^{-6}	1.2×10^{-3}	4.9×10^{-8}	80
5, 9.3	0.73	2.0×10^{-6}	2.7×10^{-3}	1.5×10^{-7}	13

[a] Measured at 20 °C in 50 mM bicine buffer, 100 mM NaCl, 1% v/v acetone, 10 μM antibody 72D4 + 400 μM amine **14**. [b] Specificity constant for the bimolecular reaction of the aldehyde with the catalyst. [c] Apparent bimolecular reaction of the aldehyde with acetone under these conditions, catalyzed by both hydroxide and free amine **14**.

that the assembled catalyst was between 320 times (with aldehyde **4**) and 950 times (with aldehyde **1**) more reactive for aldolization than amine **14** alone in solution.

Michaelis–Menten kinetics were also observed with respect to all aldehydes **1**–**5** at fixed acetone and amine concentration (Table 2). The absence of substrate selectivity and the weak binding (high K_M) observed for these aldehydes is consistent with the absence of a designed aldehyde binding site in the structure of the hapten, inducing the antibody combining site. In view of the solution chemistry of amine **14**, it is probable that the observed preequilibirum binding (K_M) of the aldehydes reflects a competitive inhibition effect by the corresponding imines (*e.g.* **16**) and that productive binding of the aldehyde is negligible. This hypothesis is supported by the similarity of the specificity constants k_{cat}/K_M with the different aldehydes. The efficiency of the antibody–amine complex with each aldehyde is given by the effective molarity k_{cat}/k_{uncat}. The rate constant k_{uncat} represents the bimolecular reaction of acetone with each aldehyde under both hydroxide and amine **14** catalysis under the reaction conditions.

The stability of the catalyst depended strongly on the concentration of acetone, as determined by Michaelis–Menten kinetics with amine **14** at fixed concentration of aldehyde **1** (200 μM). At pH 8.0, stability decreased from K_D(**14**) = 340 μM at 1% v/v acetone to K_D(**14**) = 1020 μM at 4% v/v acetone. The catalyst was completely unstable

(17) (a) Lerner, R. A.; Benkovic, S. J.; Schultz, P. G. *Science* **1991**, *252*, 659–667. (b) Schultz, P. G.; Lerner, R. A. *Acc. Chem. Res.* **1993**, *26*, 391.

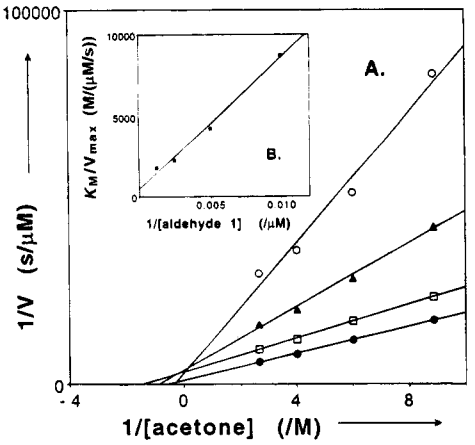

Figure 5. Catalysis of the aldol addition of acetone to aldehyde **1** by the complex of antibody 72D4 (anti-**19**) and amine **14**. (A) Double reciprocal plots of the apparent catalytic rate as a function of acetone concentration, with [aldehyde **1**] = 100 μM (○), 200 μM (▲), 400 μM (□), 820 μM (●). (B) Replot of the slopes of A versus 1/[**1**]. The slope of this line gives $\alpha \times K_M$(acetone) $\times K_M$(**1**) $\times k_{cat}^{-1} \times$ [Ab]$^{-1}$. Measured at 20 °C in 50 mM bicine, 100 mM NaCl, pH 9.2, with 18 μM antibody 72D4 and 1 mM amine **14**.

at 8% v/v acetone (K_D(**14**) > 5 mM). Stability increased at higher pH, with K_D(**14**) = 220 μM with 1.7% v/v acetone, pH 9.0, and K_D(**14**) = 130 μM with 0.5% v/v acetone, pH 9.0.

Steady state kinetic analysis with respect to aldehyde **1** and acetone was carried out at pH 9.2 at a saturating concentration of amine **14** (1 mM), and 0.9% v/v < [acetone] < 3% v/v, under which conditions the antibody–amine catalyst was expected to be fully assembled. Catalysis followed a random bimolecular model (Figure 5).[18] While preequilibrium binding was observed for aldehyde **1** (K_M(**1**) = 1700 μM), there was only a very weak binding for acetone, precluding a precise determination of its dissociation constant (K_M(acetone) > 1 M, or 7% v/v) as well as of the maximum velocity V_{max} for the catalyst. Under these nonsaturating conditions, the efficiency of the catalyst was given by the specificity constant $k_{cat}/(\alpha \times K_M(\mathbf{1}) \times K_M(\text{acetone})) = 0.068\ M^{-2}\ s^{-1}$, with [Ab]$k_{cat} = V_{max}$, obtained as the reciprocal of the slope in the replot of the slopes (Figure 5B).

We investigated the pH dependence of the catalysis by carrying out Michaelis–Menten kinetics with respect to amine **14** at a fixed, nonsaturating concentration of acetone (1% v/v) and aldehyde **1** (200 μM), between pH 8.0 and 9.7 (Figure 1). Within that range catalyst stability changed from K_D(**14**) = 400 μM at pH 7.9 to K_D(**14**) = 100 μM at pH 9.6. The data obtained for the apparent k_{cat} are consistent with the free base being the catalytically active form of the antibody–amine complex and give pK_a = 9.1 for the dissociation constant of the protonated amine **14** within the complex. This suggests that the higher reactivity of the antibody–amine complex for aldolization, as compared to the free amine in solution, is not caused by a lowering of the pK_a of the amine.

The maximum apparent specificity constant obtained for the antibody–free amine complex, k_{max}(Ab72D4 + amine **14**) = 0.123 $M^{-2}\ s^{-1}$, is in good agreement with the data from the two-dimensional plot at pH 9.2 (Figure 5). It can be compared to the maximum catalytic rate for the free amine **14**, k_{max}(**14**) = $2.0 \times 10^{-4}\ M^{-2}\ s^{-1}$. Thus the antibody–amine catalyst is approximately 600 times more reactive than amine **14** alone for catalyzing the aldolization of **1** and acetone. This magnitude seems to be valid throughout the pH range studied, for example the apparent reactivity ratio is 950 at pH 8.0, as obtained from the determination of K_D(**14**) (Figure 2).

Catalytic Mechanism. The direct precursor of enamine **III** is imminium ion **II**, whose existence is established by the isolation of the Strecker product **17**. Evidence that the antibody–amine catalyst functioned by the same enamine mechanism was provided by the observation that the antibody catalyzed the formation of amino nitrile **17** from amine **14** in the presence of cyanide and acetone, with $k_{cat} = 0.012\ s^{-1}$ and K_M = 130 μM (pH 9.0, 1% v/v acetone, 0.2 M CN^-, under these conditions $k_{uncat} = 3.8 \times 10^{-4}\ s^{-1}$). The catalytic activity was quantitatively inhibited by addition of hapten **22**, showing that the observed catalysis was taking place in the antibody combining site. Since the rate-limiting step for this reaction is the dehydration of aminal **I** to form imminium **II**,[19] this catalysis implied that the latter intermediate could form within the antibody binding site. Further evidence for an enamine mechanism with the antibody reaction was provided by the fact that secondary amine **15** + antibody 72D4 was not an active catalyst.

Chemo- and Stereoselectivity of the Antibody–Amine Catalyst. The entire undertaking of assembling an active antibody–amine catalyst for an aldol reaction is aimed at providing the reaction with chemo- and stereoselectivity. The performance of the antibody 72D4–amine **14** catalyst in that respect was demonstrated by the analysis of the reaction products. First, the catalyst was chemoselective for the formation of the aldol products. The formation of α,β-unsaturated ketones (*e.g.* **11**), which was catalyzed by amine **14** alone, was not catalyzed by the antibody–amine complex. The catalyst was also chemoselective with respect to the ketone. Aldolization of aldehyde **1** with 2-butanone or 3-pentanone was not catalyzed by the complex, despite of the fact that these reactions were catalyzed by amine **14** alone.

The stereoselectivity of the aldol reaction was investigated for aldehyde **1**. Both enantiomers of aldehyde **1** are in rapid equilibrium via enolization under the reaction conditions. Since each enantiomer can give two stereoisomeric aldol products, aldol **6** consists of four isomers. These could easily be separated by the use of chiral HPLC columns. Single isomers of aldol **6** were assigned to either enantiomer of the original aldehyde **1** by acid-catalyzed dehydration to the corresponding enone **11**. The reaction took place without racemization at the homobenzylic chiral center, and each enantiomer of enone **11** could in turn be identified by chiral column HPLC (Scheme 4).

For the reaction catalyzed either by hydroxide or by amine **14** alone, the stereoselectivity of the aldol reaction was 1.5–1. We assigned Cram-sense stereochemistry to

(18) In this model, preequilibrium binding of both substrates is followed by the catalytic step, as shown. For a complete discussion, see: Segel, I. H. *Enzyme Kinetics*; John Wiley & Sons: New York, 1975; pp 273–283.

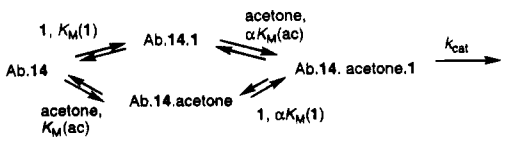

(19) Jencks, W. P. *Catalysis in Chemistry and Enzymology*; McGraw Hill: New York, 1969; pp 490–496.

Scheme 4. Catalyst Controlled *si*-Enantioselective Aldolization Using the Complex of Amine 14 plus Antibody 72D4 (anti-19)

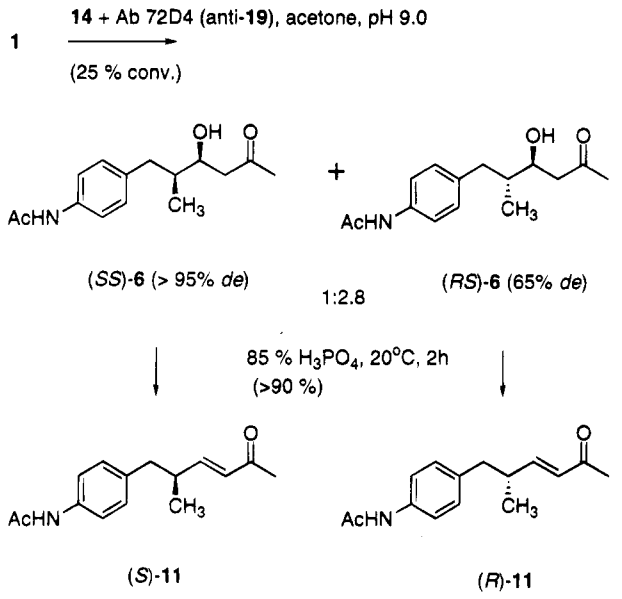

the major stereoisomer by analogy to the results reported by Heathcock *et al.* for a very similar system.[20] A semipreparative experiment was then carried out with antibody 72D4 + amine **14** and aldehyde **1** (0.2 mL, 40 μM Ab 72D4, 300 μM **1**, 300 μM amine **14**, 1% v/v acetone, pH 9.0, 20 °C). The aldol product **6** was isolated by reverse phase HPLC after 25% conversion (vs 1.8% in a control experiment under identical conditions without the antibody) and analyzed by HPLC on chiral columns. The aldol product consisted of a 1:2.8 mixture of (*SS**)-**6** (> 95% de) and (*RS**)-**6** (65% de). (*SS*)-**6** is formed by a Cram selective addition to (*S*)-**1**, while (*RS*)-**6** is formed by an anti-Cram selective addition to (*R*)-**1**. The antibody–amine complex thus selectively catalyzed addition to the *si* stereoface of the aldehyde, irrespective of the absolute configuration of the adjacent center, representing a case of reagent-controlled stereoselection.

Although the level of stereocontrol is far from perfect, it is apparent that the chiral environment of the protein brings about significant asymmetric induction to the antibody–amine complex as catalyst. Since preequilibirum binding of the aldehyde is weak, this stereoselection might be mediated by restrictive interactions which limit the number of accessible orientations for the aldehyde group within the antibody binding site.

Conclusion

We have shown catalysis of a cross-aldolization between acetone and aldehydes using simple primary amines via enamine chemistry. Although condensation of the amine catalyst with the aldehyde to form an imine, *e.g.* **16**, is inhibitory, it does not interfere at low concentrations and leaves both the amine free to form the enamine with the ketone and the aldehyde free to react as electrophile. Enamine chemistry turns out to be perhaps the only way to catalyze the reaction in water, because enolization of the ketone, which would be catalyzed by simple general bases, is a fast preequilibrium step not involved in the rate-limiting carbon–carbon bond formation. Furthermore, the spontaneous formation of the *gem*-diol form of the aldehyde in water suggests that electrophilic activation of the aldehyde would simultaneously lead to a higher proportion of the unreactive *gem*-diol form, with no net gain on catalysis. These experiments furnish a basic understanding of aqueous catalytic enamine chemistry applied to a cross-aldolization, both in terms of mechanism and scope of the reaction.

We have also demonstrated the assembly of an artificial aldolase from a primary amine and an antibody raised against the corresponding quaternary ammonium cation. At that stage the origin of the reactivity enhancement of amine **14** within the complex is not clear. While the pK of the amine does not change upon complexation, catalysis of the formation of **17** suggests that an alteration of the condensation equilibrium of acetone with amine **14** is involved in catalysis. Preequilibrium binding of acetone or the aldehyde, although apparently weak, should also contribute to catalysis by an entropy trap effect, since reaching the transition state represents a trimolecular condensation between acetone, the amine, and the aldehyde. In any event, the important point is that assembly of amine **14** with a tailored antibody results in an artificial aldolase of significantly higher reactivity and displaying good levels of stereo- and chemoselectivity.

Experimental Section

A. Synthesis. Reagents were purchased from Aldrich or Fluka. Solvents were A.C.S. grade from Fisher. All chromatographies (flash) were performed with Merck silica gel 60 (0.040–0.063 mm). Preparative HPLC was done with Fisher Optima grade acetonitrile and ordinary deionized water using a Waters prepak cartridge 500 g installed on a Waters Prep LC 4000 system from Millipore, flow rate 100 mL/min, gradient + 0.5%/min CH_3CN, detection by UV at 254 nm. TLC were performed with fluorescent F254 glass plates. MS, HRMS (high-resolution mass spectra), and combustion analyses were provided by the Scripps Research Institute facility (Gary Szuidak). J values are in hertz.

***N*-(Hydroxyethyl)-4-(aminomethyl)benzamide (14).** Gaseous hydrochloric acid was bubbled for 5 min through a suspension of 4-(aminomethyl)benzoic acid (20 mmol) in 100 mL of methanol, upon which it dissolved. After 10 min of heating at reflux, a precipitate was formed which was filtered off and washed with diethyl ether to yield 2.5 g (12.4 mmol, 62%) of 4-(carbomethoxy)benzylammonium chloride. A solution of 1.5 g of this compound in 10 mL of ethanolamine was heated at 37 °C overnight. After removal of the solvent by vacuum distillation, the residue was dissolved in 300 mL of water and treated with 50 g of Dowex H^+ (SO_3H). The resin was washed several times with water and 50% aqueous methanol. Treatment of the resin with 5% aqueous ammonia yielded 1.0 g (5.15 mmol, 69%) of amine **7** as a yellow solid, mp 140–143 °C. A sample (approximately 100 mg) was further purified by preparative reverse phase HPLC to give the pure trifluoroacetate salt as a colorless solid after lyophilization. ^{1}H-NMR (500 MHz, D_2O, **7**H^+TFA^-): 7.83, 7.56 (2d, 2 × 2H, J = 8.3); 4.26 (s, 2H); 3.78 (t, 2H, J = 5.5); 3.55 (t, 2H, J = 5.5). ^{13}C-NMR (125 MHz, D_2O, **7**H^+TFA^-): 171.6, 137.4, 135.4, 130.0, 128.9, 61.0, 43.6, 43.0. HRMS: $C_{10}H_{14}N_2O_2$, (M + H^+) calcd 195.1134, found 195.1130. IR (KBr): 3359, 3071, 2971, 2922, 2851, 2763, 1639, 1558, 1509, 1444, 1330, 1296, 1057, 962, 744, 643.

4-(3′-oxo-2′-methylprop-1′-yl)acetanilide (1). 4-Iodoacetanilide (2.19 g, 8.4 mmol), 2 mL of 2-methyl-2-propen-1-ol, 0.8 g of $NaHCO_3$, and 5 mg of palladium(II) dichloride in 5

(20) (a) Cram, D. J.; Abd Elhafez, F. A. *J. Am. Chem. Soc.* **1952**, *74*, 5828. (b) Heathcock, C. H.; Flippin, L. A. *J. Am. Chem. Soc.* **1983**, *105*, 1667. (c) Heathcock, C. *Science* **1981**, *214*, 395. The absolute configuration of aldehyde **1** has not been determined. Chirality sense is assigned to facilitate the discussion (*R*) sense chirality is given to the first peak in the chiral HPLC trace of enone **11**).

mL of *N*-methylpyrrolidone were heated at 150 °C under argon for 1 h. After workup (ethyl acetate/water), the residue was purified by chromatography (100 g of SiO_2, ethyl acetate/hexane 1.5:1, R_f = 0.25) to give 1.4 g (6.8 mmol, 81%) of aldehyde **1** as a colorless crystalline solid, mp 108–109 °C. ^{1}H-NMR (300 MHz, $CDCl_3$): 9.75 (s, 1H); 7.42, 7.14 (2d, 2 × 2H, J = 7.2); 7.20 (s, 1H); 3.62 (dd, 1H, J = 13.0, 5.7); 3.06 (dd, 1H, J = 13.0, 5.5); 3.60 (m, 1H); 2.18 (s, 3H); 1.09 (d, 3H, J = 7.0). ^{13}C-NMR (125 MHz, $CDCl_3$): 204.6, 168.7, 136.4, 134.6, 129.4, 120.2, 48.0, 36.0, 24.4, 13.1. HRMS: $C_{12}H_{15}NO_2$ (M + H$^+$) calcd 206.1181, found 206.1178. IR (KBr): 3285, 2950, 2800, 1730, 1662, 1612, 1557, 1513, 1412, 1371, 1326, 846, 773.

4-(3′-Oxoprop-1′-yl)acetanilide (2). A solution of 4-iodoacetanilide (0.9 g, 4.1 mmol) and palladium(II) dichloride (7 mg) in *N*-methylpyrrolidone (2 mL) with allyl alcohol (1 mL) and $NaHCO_3$ (500 mg) was heated at 150 °C under argon for 4 h (additional 3 mg portions of $PdCl_2$ were added after each hour), diluted with ethyl acetate (100 mL) and washed with 100 mL of aqueous saturated $NaHCO_3$. Chromatography (ethyl acetate/hexane 2:1, R_f = 0.3) yielded aldehyde **2** as a pale yellow solid (400 mg, 2.1 mmol, 51%). Then 120 mg of the compound was further purified by preparative reverse phase HPLC to give 107 mg of pure **2**, mp 60–62 °C. ^{1}H-NMR (500 MHz, $CDCl_3$): 9.81 (s, 1H); 7.69 (br s, 1H); 7.41, 7.13 (2d, 2 × 2H, J = 8.3); 2.91 (t, 2H, J = 7.4); 2.76 (t, 2H, J = 7.3); 2.15 (s, 3H). ^{13}C-NMR (125 MHz, $CDCl_3$): 201.7, 168.5, 136.2, 128.8, 128.7, 120.3, 45.2, 27.4, 24.4. HRMS: $C_{11}H_{13}NO_2$ (M + H$^+$) calcd 192.1025, found 192.1030. IR (KBr): 3298, 2834, 2740, 1719, 1665, 1650, 1604, 1547, 1515, 1408, 1371, 1320, 1270.

3-(3′-Oxo-2′-methylprop-1′-yl)acetanilide (3). 3-Iodoacetanilide (0.5 g, 2.3 mmol), 0.6 mL of 2-methyl-2-propen-1-ol, 0.2 g of $NaHCO_3$, and 2 mg of palladium(II) dichloride in 1.5 mL of *N*-methylpyrrolidone were heated at 140 °C under argon for 0.5 h. After workup (ethyl acetate/water), the residue was purified by chromatography (100 g of SiO_2, ethyl acetate/hexane 1:1, R_f = 0.35) to give 270 mg (1.31 mmol, 57%) of aldehyde **3** as a colorless solid, which was further purified by preparative RP-HPLC to give 200 mg of pure, colorless solid, mp 58–60 °C. ^{1}H-NMR (500 MHz, $CDCl_3$): 9.68 (s, 1H); 7.76 (br s, 1H); 7.40 (m, 1H); 7.32 (br d, 1H, J = 8); 7.21 (t, 1H, J = 8); 6.90 (d, 1H, J = 8); 3.03 (dd, 1H, J = 14, 6); 2.66 (qt, 1H, J = 7, 7); 2.56 (dd, 1H, J = 14, 8); 2.15 (s, 3H); 1.07 (d, 3H, J = 7). ^{13}C-NMR (125 MHz, $CDCl_3$): 204.5, 168.7, 139.7, 139.1, 129.0, 124.8, 120.3, 117.9, 47.9, 36.5, 24.5, 13.2. HRMS: $C_{12}H_{15}NO_2$ (M + H$^+$) calcd 206.1181, found 206.1187. Anal. Calcd: C, 70.22; H, 7.37; N, 6.82. Found: C, 70.01; H, 7.01; N, 6.75. IR (film): 3304, 2972, 2931, 1722, 1668, 1613, 1593, 1556, 1489, 1442, 1372, 1319, 1266.

3-(3′-Oxoprop-1′-yl)acetanilide (4). A solution of 3-iodoacetanilide (2.0 g, 7.7 mmol) and palladium(II) dichloride (5 mg) in *N*-methylpyrrolidone (3 mL) with allyl alcohol (2 mL) and $NaHCO_3$ (800 mg) was heated at 160 °C under argon for 1 h (one additional 5 mg portion of $PdCl_2$ was added after 10 min). After workup (water/ethyl acetate), chromatography (ethyl acetate/hexane 2:3 to 1.5:1) yielded aldehyde **4** as a crystalline colorless solid (660 mg, 3.4 mmol, 45%), mp 53–55 °C. A 60 mg portion of this product was further purified by preparative RP-HPLC for kinetic assays. ^{1}H-NMR (500 MHz, $CDCl_3$): 9.77 (s, 1H); 8.0 (br s, 1H); 7.41 (br s, 1H); 7.31 (br d, 1H, J = 8); 7.20 (t, 1H, J = 8); 6.91 (d, 1H, J = 8); 2.89 (t, 2H, J = 7 Hz); 2.74 (t, 2H, J = 7 Hz); 2.14 (s, 3H). ^{13}C-NMR (125 MHz, $CDCl_3$): 201.7, 168.8, 141.2, 138.2, 129.0, 124.0, 119.7, 117.8, 45.0, 27.9, 24.4. HRMS: $C_{11}H_{13}NO_2$ (M + H$^+$) calcd 192.1025, found 192.1017. Anal. Calcd: C, 69.09; H, 6.85; N, 7.33. Found: C, 68.91; H, 6.61; N, 7.37. IR (film): 3306, 3147, 3084, 2930, 2826, 2728, 1722, 1667, 1651, 1614, 1556, 1488, 1443, 1371, 1319, 1268.

3-(1′-Oxo-2′-methylpent-5′-yl)acetanilide (5). A solution of aldehyde **3** (110 mg, 0.58 mmol) in 50% aqueous ethanol (17 mL) containing 1 mL of propionaldehyde was treated with 10 drops of 2 N NaOH. After 1 h, the reaction was complete by TLC. Workup (ethyl acetate/1 N HCl) followed by preparative RP-HPLC gave pure 3-(1′-oxo-2′-methylpent-2′-en-5′-yl)-acetanilide (80 mg, 0.35 mmol, 60%). Reduction with hydrogen (1 atm, Pd/C catalyst) in ethanol (6 mL) and purification by preparative HPLC yielded 57 mg (0.24 mmol, 70%) of aldehyde **5** as a colorless oil. ^{1}H-NMR (500 MHz, $CDCl_3$): 9.58 (d, 1H, J = 2); 7.75 (br s, 1H); 7.38 (br s, 1H); 7.30 (br d, 1H, J = 8); 7.20 (t, 1H, J = 8); 6.90 (d, 1H, J = 8); 2.58 (t, 2H, J = 7); 2.33 (hex d, 1H, J = 7, 2); 2.15 (s, 3H); 1.76–1.58 (m, 2H); 1.38 (m, 1H); 1.08 (d, 3H, J = 7). ^{13}C-NMR (125 MHz, $CDCl_3$): 205.3, 168.7, 142.8, 138.0, 128.8, 124.3, 119.8, 117.5, 46.1, 35.7, 29.9, 28.5, 24.5, 13.3. HRMS: $C_{14}H_{19}NO_2$ (M + H$^+$) calcd 234.1494, found 234.1483. IR (film): 3304, 2933, 1721, 1667, 1612, 1593, 1555, 1488, 1441, 1371, 1317.

Preparation of Aldols 6–10: General Procedure. The aldehyde (30–150 mg) was dissolved in acetone (1 mL) and water (4 mL), and NaOH (0.01 mL of a saturated aqueous solution) was added. After completion of the reaction (approximately 1 h at 20 °C), the solution was diluted with water, acidified to pH 2 with trifluoroacetic acid, and purified by preparative RP-HPLC. Lyophilization of the pure fractions yielded the aldol products in approximately 60–90% yields.

6-(4′-Acetamidophenyl)-4-hydroxy-5-methyl-2-hexanone (6): colorless solid, mp 62–63 °C. ^{1}H-NMR (500 MHz, $CDCl_3$): two stereoisomers in 1.4:1 ratio. Major isomer: 7.85 (s, 1H); 7.39, 7.08 (2d, 2 × 2H, J = 8.4); 3.98 (m, 1H); 3.02 (d, 1H, J = 3.0); 2.79 (dd, 1H, J = 13.5); 2.67, 2.53 (2dd, 2 × 1H, J = 17.5, 2.6); 2.39 (dd, 1H, J = 13.5, 7); 2.17, 2.15 (2s, 2 × 3H); 1.72 (m, 1H); 0.87 (d, 3H, J = 6.5). Minor isomer: 7.85 (s, 1H); 7.39, 7.07 (2d, 2 × 2H, J = 8.3); 3.88 (m, 1H); 3.22 (d, 1H, J = 3.0); 2.86 (dd, 1H, J = 13.5, 4.6); 2.64, 2.59 (2dd, 2 × 1H, J = 17.5, 9.7); 2.33 (dd, 1H, J = 13.5, 9.5); 2.20, 2.15 (2s, 2 × 3H); 1.83 (m, 1H); 0.80 (d, 3H, J = 6.8). ^{13}C-NMR (125 MHz, $CDCl_3$). Major isomer: 210.3, 168.7, 136.8, 135.8, 129.5, 120.0, 69.2, 47.4, 40.1, 38.7, 30.8, 24.3, 13.6. Minor isomer: 210.4, 168.7, 136.5, 135.8, 129.5, 120.0, 70.8, 46.6, 40.1, 37.9, 30.8, 24.3, 14.9. MS (LSI): 264 (M + H$^+$). IR (KBr): 3500–3300; 3287, 3247, 3183, 3120, 3066, 1708, 1662, 1648, 1558, 1535, 1521, 1503, 1492, 1459, 1409, 1370, 1325, 1270, 1041, 768. Anal. Calcd for $C_{15}H_{21}NO_3$: C, 68.41; H, 8.04; N, 5.32. Found: C, 68.17; H, 7.99; N, 5.16.

6-(4′-Acetamidophenyl)-4-hydroxy-2-hexanone (7): pale yellow oil. ^{1}H-NMR (500 MHz, $CDCl_3$): 8.14 (s, 1H); 7.37, 7.07 (2d, 2 × 2H, J = 8.4), 4.01 (m, 1H); 3.41 (d, 1H, J = 2.8); 2.71 (m, 1H); 2.61 (m, 3H); 2.14, 2.10 (2s, 2 × 3H); 1.74, 1.64 (2m, 2 × 1H). ^{13}C-NMR (125 MHz, $CDCl_3$): 210.0, 168.8, 137.6, 135.8, 128.7, 120.2, 66.6, 49.9, 37.9, 30.9, 30.7, 24.2. HRMS: $C_{14}H_{19}NO_3$ (M + H$^+$) calcd 250.1443, found 250.1450. IR (film): 3500–3200, 3123, 2935, 2916, 1710, 1667, 1604, 1535, 1434, 1370, 1070, 832, 733.

6-(3′-Acetamidophenyl)-4-hydroxy-5-methyl-2-hexanone (8): colorless oil, 1.5:1 mixture of stereoisomers. ^{1}H-NMR (500 MHz, $CDCl_3$). Major isomer: 8.17 (s, 1H); 7.35 (br d, 1H, J = 8); 7.32 (br s, 1H); 7.17 (br t, 1H, J = 8); 6.87 (t, 1H, J = 8); 3.97 (dt, 1 H, J = 10, 2); 3.10 (br s, 1H); 2.75 (dd, 1 H, 13, 6); 2.65–2.45 (m, 2H); 2.35 (dd, 1 H, J = 13, 8); 2.15 (s, 3H); 2.14 (s, 3H); 1.73 (m, 1 H); 0.83 (d, 3H, J = 7). Minor isomer: 8.17 (s, 1H); 7.35 (br d, 1H, J = 8); 7.32 (br s, 1H); 7.17 (br t, 1H, J = 8); 6.87 (t, 1H, J = 8); 3.87 (ddd, 1 H, J = 9, 6, 2); 3.10 (br s, 1H); 2.83 (dd, 1 H, J = 14, 5); 2.65–2.45 (m, 2H); 2.28 (dd, 1H, J = 13, 9); 1.82 (m, 1 H); 2.17 (s, 3H); 2.14 (s, 3H); 0.77 (d, 3H, J = 7). ^{13}C-NMR (125 MHz, $CDCl_3$). Major isomer: 210.3, 168.9, 141.7, 138.0, 128.7, 124.9, 120.5, 117.5, 69.2, 47.4, 39.9, 39.2, 30.7, 24.3, 13.6. Minor isomer: 210.5, 168.9, 141.4, 138.0, 128.6, 125.0, 120.5, 117.5, 70.9, 46.6, 40.0, 38.4, 30.8, 24.3, 14.9. HRMS: $C_{15}H_{21}NO_3$ (M + H$^+$) calcd 264.1600, found 264.1593. IR (film): 3309, 3149, 2965, 2930, 1704, 1667, 1613, 1592, 1556, 1489, 1434, 1372, 1317, 1268, 1168, 1103, 1058, 964, 780, 702, 537.

6-(3′-Acetamidophenyl)-4-hydroxy-2-hexanone (9): colorless oil. ^{1}H-NMR (500 MHz, $CDCl_3$): 7.70 (br s, 1H); 7.36 (br s, 1H); 7.32 (br d, 1H, J = 8); 7.20 (t, 1H, J = 8); 6.93 (d, 1H, J = 8); 4.01 (m, 1H); 3.25 (br s, 1H); 2.75 (m, 1H); 2.64 (m, 1H); 2.61 (m, 2H); 2.16 (s, 3H); 2.15 (s, 3H); 1.77 (m, 1H); 1.66 (m, 1H). ^{13}C-NMR (125 MHz, $CDCl_3$): 210.1, 168.6, 142.7, 138.0, 128.9, 124.4, 119.9, 117.5, 66.6, 49.9, 37.7, 31.6, 30.7, 24.5. HRMS: $C_{14}H_{19}NO_3$ (M + H$^+$) calcd 250.1443, found 250.1432. IR (film): 3306, 2928, 1704, 1667, 1612, 1592, 1556, 1489, 1434, 1371, 1319, 1168, 1072, 786, 699.

8-(3′-Acetamidophenyl)-4-hydroxy-5-methyl-2-octanone (10): colorless oil, 2:1 mixture of stereoisomers. ^{1}H-NMR (500 MHz, $CDCl_3$). Major isomer: 7.62 (br s, 1H); 7.35 (br s, 1H); 7.30 (br d, 1H, J = 8); 7.20 (t, 1H, J = 8); 6.91 (d, 1H, J = 8); 3.96 (dt, 1 H, J = 9, 3); 2.56 (m, 4H); 2.18 (s, 3H); 2.15 (s, 3H); 1.66 (m, 1H); 1.58 (m, 1H); 1.49 (m, 2H); 1.16 (m, 1H); 0.88 (d, 3H, J = 7). Minor isomer: 7.62 (br s, 1H); 7.35 (br s, 1H); 7.30 (br d, 1H, J = 8); 7.20 (t, 1H, J = 8); 6.91 (d, 1H, J = 8); 3.88 (m, 1 H); 2.19 (s, 3H); 2.15 (s, 3H); 1.66 (m, 1H); 1.58 (m, 1H); 1.49 (m, 2H); 1.16 (m, 1H); 0.87 (d, 3H, J = 7). ^{13}C-NMR (125 MHz, $CDCl_3$). Major isomer: 210.4, 168.5, 143.4, 137.8, 128.8, 124.4, 119.8, 117.3, 70.4, 47.1, 37.7, 35.9, 32.1, 30.8, 28.9, 24.5, 14.2. Minor isomer: 210.4, 168.5, 143.4, 137.8, 128.8, 124.4, 119.8, 117.3, 71.1, 46.3, 37.8, 35.9, 31.7, 30.8, 28.7, 24.5, 14.9. HRMS: $C_{17}H_{25}NO_3$ (M + H$^+$) calcd 292.1913, found 292.1910. IR (film): 3306, 2932, 1704, 1668, 1613, 1592, 1556, 1488, 1440, 1371, 1318, 1167, 1065, 792, 699.

Preparative Scale Reaction with Aldehyde 1 and Amine 14. Aldehyde 1 (164 mg, 0.8 mmol, final concentration 0.1 M) was dissolved in 8 mL of 50 mM bicine (adjusted to pH 8.0 with NaOH), 0.1 M amine **14**, and 0.1 M NaCl. After addition of 0.16 mL of acetone, the solution was heated at 80 °C for 5 h, cooled to room temperature, and neutralized to pH 6.6. Purification by preparative reverse phase HPLC as above yielded amine **14** (222 mg, 0.72 mmol, 90% recovery), aldol **6** (46 mg, 0.18 mmol, 23%), α,β-unsaturated ketone **11** (91 mg, 0.37 mmol, 46%), and recovered aldhyde **1** (25 mg, 15%).

6-(4′-Acetamidophenyl)-5-methyl-3-hexen-2-one (11): colorless solid, mp 57−58 °C. ^{1}H-NMR (500 MHz, $CDCl_3$): 7.58 (s, 1H); 7.42, 7.06 (2d, 2 × 2H, J = 8.3); 6.73 (dd, 1H, J = 16, 7); 5.98 (d, 1H, J = 16); 2.69 (m, 1H); 2.58 (m, 2H); 2.22, 2.16 (2s, 2 × 3H); 1.05 (d, 3H, J = 6.2). ^{13}C-NMR (125 MHz, $CDCl_3$): 198.9, 168.4, 152.5, 136.1, 135.3, 129.6, 129.4, 119.9, 41.8, 38.3, 26.9, 24.4, 18.7. HRMS: $C_{15}H_{19}NO_2$ calcd 246.1494, found 246.1490. Anal. Calcd: C, 73.44; H, 7.81; N, 5.71. Found: C, 73.50; H, 7.73; N, 5.83. IR (KBr): 3288, 3249, 1697, 1671, 1612, 1357, 1530, 1492, 1410, 1325, 1263, 985, 784.

Aldol Condensation of Aldehyde 2 Using Methylamine Catalyst. Aldehyde **2** (0.2 g, 1 mmol, final concentration 2 mM) was dissolved in 0.4 L of aqueous 50 mM phosphate buffer pH 7.4. Then 40 mL of acetone and 20 mL of 1 M methylammonium chloride (final concentration 45 mM) in water were added, and the pH was adjusted to 8.5 with NaOH. After 5 days at 20 °C, the solution was acidified to pH 6.6 with HCl, diluted to 1 L with water, and directly loaded on a preparative reverse phase HPLC column (Waters cartridge C-18, 500 g). Gradient elution (95/5 to 75/25 water/acetonitrile in 30 min, linear gradient at 100 mL/min flow rate) gave, after lyophilyzation of the collected fractions, aldol **6** (t_R = 16 min, 50 mg, 0.2 mmol, 20%), enone **12** (t_R = 26 min, 10 mg, 0.04 mmol, 4%), and unsaturated aldehyde **13** (t_R = 35 min, 20 mg of a colorless solid, mp154−156 °C, 0.055 mmol, 5.5%).

6-(4′-Acetamidophenyl)-3-hexen-2-one (12): colorless solid, mp 105−106 °C. ^{1}H-NMR (500 MHz, $CDCl_3$): 7.42, 7.13 (2d, 2 × 2H, J = 8.2); 7.21 (br s, 1H); 6.81 (ddd, 1H, J = 16, 6.8, 6.8); 6.09 (ddd, 1H, J = 16, 1.0, 1.0); 2.76 (t, 2H, J = 7); 2.54 (m, 2H); 2.55, 2.18 (2s, 2 × 3H). ^{13}C-NMR (125 MHz, $CDCl_3$): 198.5, 168.2, 147.0, 136.6, 136.0, 131.7, 128.8, 120.1, 34.1, 33.8, 26.9, 24.6. MS (LSI): 232 (M + H$^+$). IR (KBr): 3288, 3253, 1671, 1655, 1604, 1542, 1412. Anal. Calcd for $C_{14}H_{17}NO_2$: C, 72.70; H, 7.41; N, 6.06. Found: C, 72.24; H, 7.42; N, 6.02.

1,5-Bis(4′-acetamidophenyl)-2-pentene-2-carboxaldehyde (13): colorless solid, mp 154−156 °C. ^{1}H-NMR (500 MHz, $CDCl_3$): 9.43 (s, 1H); 7.61, 7.38 (2 bs, 2 × 1H); 7.31, 7.23, 6.98, 6.85 (4d, 4 × 2H, J = 8.3); 6.60 (t, J = 7.2); 3.50 (s, 2H); 2.77 (t, 2H, J = 7.0); 2.71 (dt, 2H, J = 7.2, 7.0); 2.19, 2.17 (2s, 2 × 3H). ^{13}C-NMR (125 MHz, CD_3OD): 196.6, 171.6, 171.5, 157.3, 144.2, 138.1, 138.0, 137.8, 136.4, 129.8, 129.6, 121.4, 121.3, 34.7, 32.3, 29.6, 23.7, 23.6. MS: 365 (M + H$^+$). IR (KBr): 3311, 1686, 1677, 1663, 1642, 1608, 1597, 1530, 1412, 1373, 1315.

Determination of the Stereochemistry of the Isomers of Aldol 6. Antibody Assay. A 0.2 mL portion of a buffered solution (50 mM bicine, 100 mM NaCl, pH 9.0) containing Ab 72D4 (40 μM), aldehyde **1** (300 μM), amine **14** (300 μM), and 1% v/v acetone was incubated at 20 °C for 10 days, which gave 25% conversion to aldol product **6**. Two similar solutions, one without the antibody and one with antibody 72D4 and 250 μM hapten **21**, gave only 1.8% product formation under these conditions. The aldol product was isolated by reverse phase HPLC on an analytical column (2 × 0.1 mL runs) and lyophilized. The residue was then dissolved in 3:1 hexane/2-propanol and analyzed on a chiral column (see below).

Analysis on Chiral Columns. Samples of aldol **6** collected by HPLC were used as solution in 3:1 hexane/2-propanol and analyzed on chiral HPLC columns (3/1 hexane/2-propanol, 1.0 mL/min) as follows. **6** separated on Chiracell AS: t_R((*RS*)-**6**) = 23.3 min, t_R((*SR*)-**6**) = 25.0 min, t_R((*S***S**)-**6**) = 28.9 min. The fraction at t_R = 28.9 min was collected (approximately 2 mL), concentrated by evaporation, and separated on Chiracell OJ: t_R((*SS*)-**6**) = 11.7 min, t_R((*RR*)-**6**) = 16.1 min.

Stereochemical Assignment. The stereochemistry of the individual stereoisomers of aldol **6** was assigned as follows. (a) Configuration at the methyl group. By reaction in 85% H_3PO_4 (20 °C, 2 h), each isolated **6** isomer gave cleanly and without racemization one of the enantiomers of the corresponding α,β-unsaturated ketone **11**. This product was isolated by RP-HPLC and analyzed on Chiracell AS: t_R((*R*)-**11**) = 19.1 min and t_R((*S*)-**11**) 21.9 min (chirality sense assigned arbitrarily). (b) Relative stereochemistry. Cram-sense stereochemistry was attributed to the major stereoisomer ((*S***S**)-**6**) of the background reaction (stereoselection: 1.5:1) in analogy to the observation of Heathcock *et al.* on a similar system. The absolute configuration was not determined. The numbers reported for the antibody + amine catalyst reaction refer to isomeric ratios after correction for the background reaction.

***N*-((4′-(2-hydroxyethyl)carbamoyl)phenyl)methyl)-2-amino-2-methylpropionitrile (17).** Amine **14** (30 mg of HPLC-purified TFA salt) was dissolved in water (0.5 mL) and treated with acetone (0.02 mL) and NaCN (10 mg). The pH was adjusted to 9.0 and the solution incubated overnight at 20 °C. The solution was then acidified to pH 2.0 with trifluoroacetic acid and purified by preparative HPLC. The isolated TFA salt of **17** was suitable for MS analysis. NMR spectra were collected in a solution prepared as above in D_2O. ^{1}H-NMR (500 MHz, D_2O): 7.77, 7.47 (2d, 2 × 2H, J = 8); 3.88 (s, 2H); 3.78 (t, 2H, J = 5.5); 3.54 (t, 2H, J = 5.5); 1.57 (s, 6H). HRMS: observed $C_{13}H_{18}N_2O_2$ (loss of HCN), (M + H$^+$) calcd 235.1447, found 235.1453. ^{13}C-NMR (125 MHz, D_2O): 170.0, 141.6, 133.4, 132.2, 127.0, 122.6, 114.7, 59.5, 51.0, 47.8, 25.3.

Detection of Imine 16 in Aqueous Solutions. Imine **16** forms spontaneously in a buffered solution of amine **14** in water at basic pH and can be detected by RP-HPLC (t_R = 11.5 min, conditions of aldehyde **1** in Table 1). The mass spectrum of a 50 mM solution of amine **14** and aldehyde **1** buffered at pH 9.0, with 10% acetonitrile as cosolvent, shows a major peak at 382. **16**: $C_{22}H_{27}N_3O_7$, HRMS (M + H$^+$) calcd 382.2131, found 382.2129. In D_2O at pD 9.0, a mixture of 10 mM amine **14** and 5 mM aldehyde **1** consists of a 1:3:3 equilibrium mixture of imine **16**, aldehyde **1**, and its corresponding hydrated form (*gem*-diol). ^{1}H-NMR (300 MHz, D_2O). **1:** 7.26, 7.22 (2d, 2 × 2H, J = 8); 3.00 (dd, 1H, J = 14, 7); 2.66 (dd, 1H, J = 14, 8); 2.15 (s, 3H); 1.90 (m, 1H); 1.00 (d, 3H, J = 7). Visible signals for *gem*-diol: 2.83 (dd, 1H, J = 14, 6); 2.38 (dd, 1H, J = 14, 9); 0.80 (d, 3H, J = 7). For imine **16**: 7.58, 7.16, 7.10, 6.95 (4d, 4 × 2H, J = 8); 4.55, 4.25 (2d, 2 × 1H, J = 12); 1.08 (d, 3H, J = 7).

B. Kinetic Measurements. Aldehydes **1**−**5** were used as 25 mM stock solutions of the RP-HPLC purified samples in 1:1 acetonitrile/water. Amine **14** was used as a 25 mM stock solution of the RP-HPLC purified trifluoroacetate salt in pure water. Antibody 72D4 was purified to homogeneity (SDS PAGE) by ion exchange and Protein G chromatography as described before, at 8−12 mg/mL stock solutions in either bicine (50 mM, pH 8.0) or phosphate (50 mM, pH 7.4) with 100 mM NaCl.

Assay Setup. The setup for the kinetics of Figure 4 is representative: a stock solution (1.8 mL) containing the antibody (11.1 μM) and acetone (1.11% v/v) in 50 mM bicine, 100 mM NaCl, pH 8.0, was separated into four portions of 400 μL. To each was added 3.6 μL of a 25 mM stock solution of

each of the aldehydes **1** to **4**. Each 400 μL portion was further separated into four 90 μL portions, and 10 μL solutions of amine **14** in 50 mM bicine, 100 mM NaCl (1 mM, 2 mM, 4 mM, 8 mM), were added. Finally, 50 μL of each 100 μL sample was added to 0.5 μL of a 25 mM stock solution of hapten **22** in water. In each manipulation, the samples were vigorously shaken using a Vortex shaker to ensure homogeneity (shaking has no adverse effect on antibody activity). The solutions obtained contained 200 μM each aldehyde, 100, 200, 400, and 800 μM amine **14**, 10 μM antibody 72D4, and 1% v/v acetone in the buffer with or without 250 μM hapten **22** and were in 0.5 mL plastic Eppendorf tubes. These samples were incubated at 20 °C in a closed box containing 1% v/v acetone in water to prevent evaporation of the acetone. The samples with antibody plus inhibitor were used for the uncatalyzed reaction, and the samples with antibody only for the catalyzed reaction, under each concentration conditions.

HPLC Assays. Product formation below 5% conversion versus starting material was followed over time by reverse phase HPLC using a 5 μM, 300 Å pore size C-18 silica column (0.45 × 22 cm) under isocratic elution conditions with an acetonitrile/water mixture at 1.5 mL/min (Table 1), detection by UV at 250 nm. The signal was recorded on a digital integrator.

Data Treatment. The initial apparent first-order rates in the inhibited antibody samples were used as measurements of the background reaction rate. The plot of this background rate versus amine **14** concentration was linear (four points, $r^2 > 0.995$) and gave the hydroxide-catalyzed reaction as the y-intercept and the apparent reaction rate for the amine-catalyzed reaction at that pH as the slope (see Figure 1 and text). The net catalytic rate in each antibody assay was obtained by subtracting the observed background rate in the corresponding inhibited sample. The net rates were used to derive the Michaelis–Menten constant K_M and the maximum velocity V_{max} from the Lineweaver–Burke plot of $1/V$ versus 1/[S] (four points, $r^2 > 0.993$). The catalytic constant k_{cat} was obtained by dividing V_{max} by the observed concentration of active catalytic sites in the antibody sample, which was determined by quantitative titration with hapten **22** as described before. This measurment is accurate to within ±10%. Although the scatter of the data obtained in these measurments is very small ($r^2 > 0.99$), fluctuations in room temperature and HPLC conditions can be the source of systematic errors, implying that the rate constants determined here should be taken with an error margin of ±15%.

Formation of α-Aminonitrile 17. Conditions: 50 mM bicine, 0.2 M NaCN, pH 9.0, 20 °C, 50–1600 μM **14**, 1% v/v acetone, 10 μM antibody 72D4. The reaction was initiated by addition of a concentrated stock solution of either amine **14** or NaCN (adjusted to pH 9.0 with HCl). (Warning! Buffered cyanide solutions slowly release HCN and should be handled in a fume hood.) As above, pairs of identical antibody solutions, with and without hapten **22** as inhibitor, were used for measuring the background and catalyzed reaction rates, respectively. Samples (15 μL) were quenched at 45 s intervals by being mixed with 15 μL of 0.5 N TFA in water, immediately frozen, and later analyzed by RP-HPLC (C-18 as above, 92.5% H_2O, 7.5% CH_3CN, t_R(**17**) = 7.8 min) against an internal standard (4-hydroxybenzoic acid, t_R = 9.4 min). A large injection peak caused by cyanide masked the peak for amine **14** (t_R = 3.4 min) under these conditions. The background rate k_{uncat} was derived from the inhibited samples (V versus [S], six points, $r^2 = 1.0$). K_M and V_{max} were obtained from the Lineweaver–Burk plot of 1/V versus 1/[S] as above (50, 100, 200, 400, 800, 1600 μM **14**, six points, $r^2 = 0.98$).

Enolization of Acetone in D_2O. Two 100 mM stock solutions of either amine **14** TFA salt or N-methyldiethanolamine were adjusted at pD = 9.0 (electrode reading 8.6)[21] and diluted with 100 mM NaCl in D_2O to obtain final concentrations of 10, 15, 20, 25, and 30 mM of the amine. The pD of all these solutions was 9.0 ± 0.05. Acetone-d_0 was added to make 1% v/v, and the decrease of the integration of the acetone ^{1}H-signal, versus the signals of the amines, was followed over time. The reaction was followed for 2 half-lives and showed first-order kinetics over that period. The rate of proton exchange at [amine] = 0 was extrapolated from the rate measured with N-methyldiethanolamine.

Solutions were similarly prepared containing 0 or 2 mM amine **14**, with 200 μM aldehyde **1**, 3% v/v acetone, and 25, 50 or 75 mM N-methyldiethanolamine at pD = 9.0, and the rate of formation of aldol **6** was measured by RP-HPLC as above. The rate of aldolization observed was independent of the concentration of N-methyldiethanolamine with both 0 and 2 mM **10**.

Acknowledgment. We thank Prof. R. A. Lerner for his help and suggestions. This work was supported by the National Institutes of Health (GM49736 to J.-L. R.).

Supporting Information Available: HPLC traces of the separation on reverse phase and chiral phase columns for aldol **6** and ^{1}H-NMR spectra of compounds **1-14**, **16**, and **17** (22 pages). This material is contained in libraries on microfiche, immediately follows this article in the microfilm version of the journal, and can be ordered from the ACS; see any current masthead page for ordering information.

JO950836Y

(21) (a) Clascoe, P. K.; Long, F. A. *J. Phys. Chem.* **1960**, *64*, 188. (b) Bell, R. P.; Kuhn, A. T. *Trans. Faraday Soc.* **1963**, *59*, 1789.